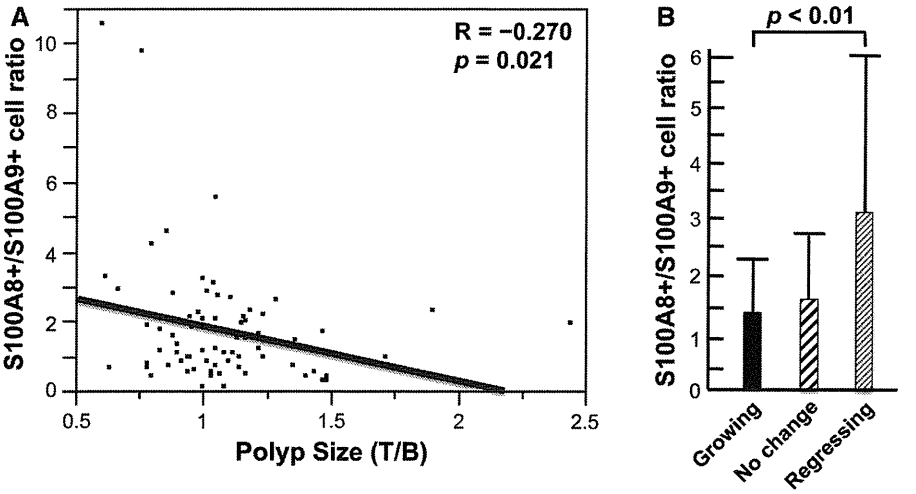

Fig. 7 Polyp-associated S100A8+ and S100A9+ cells and polyp growth. At the end of the trial, a final colonoscopic examination was performed. All target polyps were then removed and processed for histological examination. 91 polyps were histologically diagnosed. The density of S100A8+ cells and S100A9+ cells could be determined by immunohistochemistry in 72 of these polyps: 29 participants had target polyps that had increased in size by 10 % or more (growing polyps), 16 participants had target polyps that had decreased in size by 10 % or more (regressing polyps), and the remaining 27 participants had polyps that were diagnosed as having no change in size. **a** There was a significant inverse correlation between polyp size and the ratio of S100A8+/S100A9+ cells in the polyps. **b** The ratio of S100A8+/S100A9+ cells was significantly higher in regressing polyps compared to growing polyps

collection procedures are consistent with the premise that ingestion of bLF promotes immune function by priming immune effector cells.

Polyp-associated CD4+ cells

There was a significant increase in CD4+ cells in the polyps of trial participants ingesting 3.0 g bLF (Fig. 10). A likely cause of the increased number of CD4+ in these polyps is induction of cytokine expression in the colons of trial participants ingesting 3.0 g bLF: Using the RNA extracted from the normal mucosal samples collected prior to the beginning and at the end of the trial, we found that ingestion of 3.0 g bLF resulted in an increase of IFNA expression in the colon mucosa (Alexander et al. submitted). These findings are consistent with the increase of peritumoral and intratumoral CD4+ cells 15 days after intralesional injection of basal cell carcinomas with IFNA (Mozzanica et al. 1990) and suggest that induction of IFNA in the colons of participants ingesting 3.0 g bLF resulted in an increase of CD4+ cells in the colon mucosa and, consequently, in the colorectal polyps of these trial participants.

Polyp-associated CD161+ cells

There was also a significant increase of CD161+ cells (primarily NK cells) in the polyps of trial participants ingesting 3.0 g bLF (Fig. 11). It is likely that the increased number of NK cells in these polyps is also caused by bLF-mediated induction of cytokine expression in the colons of these trial participants: IFNA induces expression of CXCL10 (Lande et al. 2003), and CXCL10 is chemotactic for NK cells (Lande et al. 2003; Megjugorac et al. 2004). It is important to note that increased infiltration of NK cells into the polyps of participants ingesting 3.0 g bLF is not equivalent to an increased presence of NK cells in regressing polyps. As discussed above, in the absence of other factors, immune cells involved in immunosurveillance and removal of transformed cells, such as NK cells, will be present in polyps only briefly, as tumorigenic cells are being targeted. However, increased numbers of NK cells in a polyp will enhance the ability of the immune system to target and remove transformed cells in that polyp.

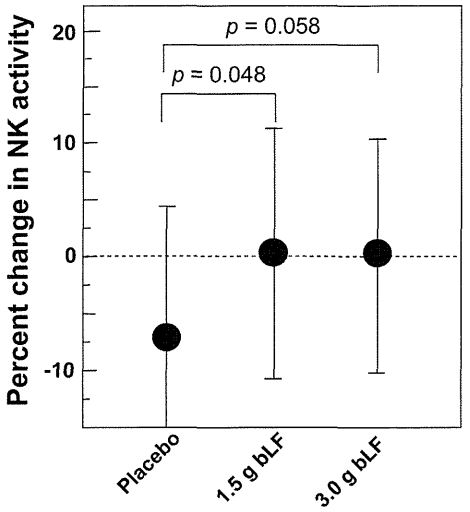

Fig. 8 Effect of bLF on systemic NK cell activity. The change in NK activity in peripheral blood samples measured prior to the beginning and at the end of the trial is shown. There were 33 patients in the placebo group, 37 patients in the 1.5 g bLF group, and 32 patients in the 3.0 g bLF group. The relative change in NK activity in the blood of the trial participants at the end of the one-year trial period was significantly higher in the 1.5 g bLF group compared the placebo group; however, the relative change in the 3.0 g bLF group was not significantly increased compared to the placebo group. This figure is adapted from Fig. 2, Kozu et al. (2009), Effect of Orally Administered Bovine Lactoferrin on the Growth of Adenomatous Colorectal Polyps in a Randomized, Placebo-Controlled Clinical Trial

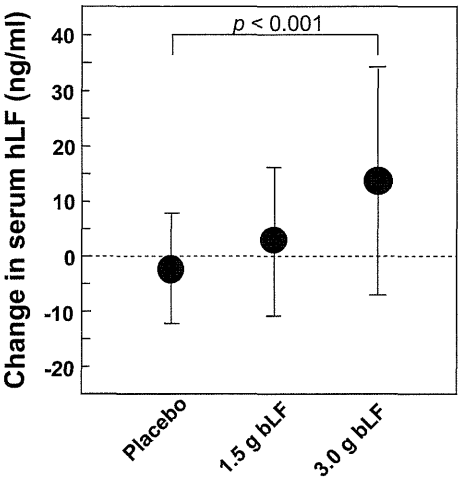

Fig. 9 Effect of bLF on serum hLF levels. The change in hLF levels in serum samples measured prior to the beginning of the trial and at the end of the trial are shown. There were 33 patients in the placebo group, 37 patients in the 1.5 g bLF group, and 32 patients in the 3.0 g bLF group. The levels of serum hLF at the end of the one-year trial period was significantly higher in the 3.0 g bLF group compared the placebo group. This figure is adapted from Fig. 1, Kozu et al. (2009), Effect of Orally Administered Bovine Lactoferrin on the Growth of Adenomatous Colorectal Polyps in a Randomized, Placebo-Controlled Clinical Trial

Polyp associated PMNs, CD66b+, S100A8+ and S100A9+ cells

There was no significant net effect on the presence of PMNs, CD66+ cells, S100A8+ cells or S100A9+ cells in the polyps of trial participants ingesting 3.0 g bLF (data not shown). This result suggests that ingestion of bLF had little effect on the inflammatory potential of the colon mucosa.

Summary and conclusions

The data presented in this report show a good correlation between increased levels of NK cell activity in the blood, increased levels of serum hLF, which reflects systemic neutrophil responsiveness, and regression of colorectal polyps. These data are consistent with a correlation between higher immune system activity and suppression of colorectal polyps.

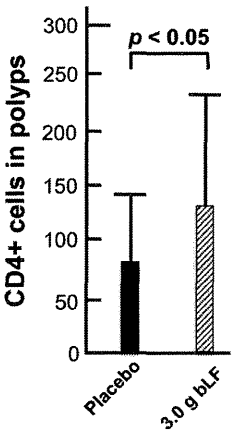

Fig. 10 Effect of bLF on polyp-associated CD4+ cells. At the end of the trial, a final colonoscopic examination was performed. All target polyps were then removed and processed for histological examination. 91 polyps were histologically diagnosed, and the density of CD4+ cells was determined in 37 polyps from the placebo group and 37 polyps from the 3.0 g bLF group. There was a significant increase in CD4+ cells in the polyps from the 3.0 g bLF group compared to the placebo group

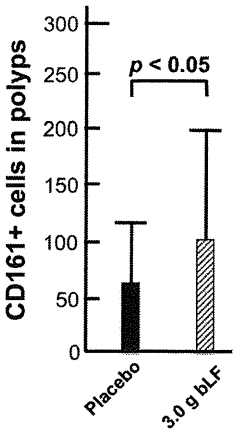

Fig. 11 Effect of bLF on polyp-associated CD161+ cells. At the end of the trial, a final colonoscopic examination was performed. All target polyps were then removed and processed for histological examination. 91 polyps were histologically diagnosed, and the density of CD161+ cells was determined in 37 polyps from the placebo group and 35 polyps from the 3.0 g bLF group. There was a significant increase in CD161+ cells in the polyps from the 3.0 g bLF group compared to the placebo group

Our data also show a good correlation between the presence of CD4+ cells in colorectal polyps and regressing polyps. This finding is consistent with the key role CD4+ cells have in immune system function and is also consistent with a correlation between higher immune system activity and suppression of colorectal polyps. In addition, our data support the proposal that lower inflammatory potential in the colon mucosa, as manifested by decreased numbers of neutrophils and increased numbers of S100A8+ cells, is associated with suppression of colorectal polyps.

Ingestion of bLF caused a possible marginal increase in systemic NK cell activity and a significant increase in serum hLF levels. These findings are consistent with the presence of primed NK cells and neutrophils in the serum. In addition, ingestion of bLF resulted in an increase in the number of CD4+ and NK cells in colorectal polyps. Notably, the colorectal polyps examined in the Tokyo trial persisted throughout the one-year trial period in the patients ingesting 3 g bLF daily, indicating that the polyp-associated CD4+ and NK did not induce an immune response against the polyps. This also consistent with the suggestion that ingestion of bLF primed rather than activated immune effector cells. This premise would predict that ingestion of bLF would not change immune function from OFF to ON, but rather immune function would change from a less responsive state to a more responsive state. Thus, the presence of CD4+ cells and NK cells in polyps without transformed cells would enhance targeting of cells once they acquire a transformed phenotype, thereby decreasing polyp growth. Taken together, our findings are consistent with the proposition that ingestion of bLF suppressed colorectal polyps by enhancing immune system responsiveness.

As previously reported by Kozu et al. (2009), trial participants 63 years old and younger ingesting 3.0 g bLF daily for one year had a statistically significant regression in the growth of colorectal polyps compared with participants ingesting placebo, however, bLF had no significant effect on polyps in participants 64 years old and older. This suggests that while ingestion of bLF resulted in suppression of colorectal polyps, an age related factor affected the trial participants' response to bLF. One possibility is that to generate an effect, bLF must be digested into peptide fragments, and decreased digestive capability in some of the older trial participants resulted in decreased suppression of colorectal polyps in these individuals. Another possibility, is that immune responsiveness was influenced by the inflammatory potential of the colon mucosa, and the inflammatory potential of the colon mucosa of some of the older trial participants was strong enough to counter the effects of bLF.

As noted above, the colorectal polyps examined in the Tokyo trial persisted throughout the one-year trial period in the patients ingesting 3 g bLF daily. A crucial conclusion that can be drawn from this fact is that bLF did not induce an immune response against the polyps. This is a physiologically reasonable and key consideration: The cells in these polyps were mostly pre-cancerous and, consequently, were essentially normal. Lack of an immune response against these cells indicates that the increased responsiveness of immune effector cells in the trial participants ingesting 3.0 g bLF did not result in an autoimmune response. Importantly, in all of the animal and human studies conducted to date, which include chronic administration to animals and daily intake for one year by human patients, ingestion of bLF has been shown to be toxicologically safe.

Acknowledgments This study was partly funded by The Princess Takamarsu Cancer Research Fund and Morinaga Milk Industry Co., Ltd (Tokyo, Japan). We thank Takayuki Akasu

and Takuji Gotoda of the Endoscopic Data-Adjudication Committee, Tadakazu Shimoda, a pathologist, and Takahiro Fujii, an endoscopist (until June 2003). We also thank DIMS institute for technical assistance.

References

Alexander DB, Iigo M, Yamauchi K, Suzui M, Tsuda H (2012) Lactoferrin: an alternative view of its role in human biological fluids. Biochem Cell Biol 90(3):279–306. doi:10.1139/o2012-013

Ambruso DR, Sasada M, Nishiyama H, Kubo A, Komiyama A, Allen RH (1984) Defective bactericidal activity and absence of specific granules in neutrophils from a patient with recurrent bacterial infections. J Clin Immunol 4(1):23–30

Anceriz N, Vandal K, Tessier PA (2007) S100A9 mediates neutrophil adhesion to fibronectin through activation of beta2 integrins. Biochem Biophys Res Commun 354(1):84–89. doi:10.1016/j.bbrc.2006.12.203

Balkwill F, Mantovani A (2001) Inflammation and cancer: back to Virchow? Lancet 357(9255):539–545. doi:10.1016/S0140-6736(00)04046-0

Bhatnagar N, Hong HS, Krishnaswamy JK, Haghikia A, Behrens GM, Schmidt RE, Jacobs R (2010) Cytokine-activated NK cells inhibit PMN apoptosis and preserve their functional capacity. Blood 116(8):1308–1316. doi:10.1182/blood-2010-01-264903

Brown RD, Rickard KA, Kronenberg H (1983) Immunoradiometric assay of plasma lactoferrin. Pathology 15(1):27–31

Brown RD, Yuen E, Rickard KA, Vincent PC, Young G, Kronenberg H (1986) Plasma lactoferrin in patients with neutropenia. Blut 52(5):289–295

Donato R, Cannon BR, Sorci G, Riuzzi F, Hsu K, Weber DJ, Geczy CL (2013) Functions of S100 proteins. Curr Mol Med 13(1):24–57

Freitas M, Porto G, Lima JL, Fernandes E (2008) Isolation and activation of human neutrophils in vitro. The importance of the anticoagulant used during blood collection. Clin Biochem 41(7–8):570–575. doi:10.1016/j.clinbiochem.2007.12.021

Gebhardt C, Nemeth J, Angel P, Hess J (2006) S100A8 and S100A9 in inflammation and cancer. Biochem Pharmacol 72(11):1622–1631. doi:10.1016/j.bcp.2006.05.017

Gessler P, Pretre R, Hohl V, Rousson V, Fischer J, Dahinden C (2004) CXC-chemokine stimulation of neutrophils correlates with plasma levels of myeloperoxidase and lactoferrin and contributes to clinical outcome after pediatric cardiac surgery. Shock 22(6):513–520

Goyette J, Geczy CL (2011) Inflammation-associated S100 proteins: new mechanisms that regulate function. Amino Acids 41(4):821–842. doi:10.1007/s00726-010-0528-0

Hsu K, Passey RJ, Endoh Y, Rahimi F, Youssef P, Yen T, Geczy CL (2005) Regulation of S100A8 by glucocorticoids. J Immunol 174(4):2318–2326

Ichikawa M, Williams R, Wang L, Vogl T, Srikrishna G (2011) S100A8/A9 activate key genes and pathways in colon tumor progression. Mol Cancer Res 9(2):133–148. doi:10.1158/1541-7786.MCR-10-0394

Kozu T, Iinuma G, Ohashi Y, Saito Y, Akasu T, Saito D, Alexander DB, Iigo M, Kakizoe T, Tsuda H (2009) Effect of orally administered bovine lactoferrin on the growth of adenomatous colorectal polyps in a randomized, placebo-controlled clinical trial. Cancer Prev Res (Phila) 2(11):975–983. doi:10.1158/1940-6207.CAPR-08-0208

Lande R, Giacomini E, Grassi T, Remoli ME, Iona E, Miettinen M, Julkunen I, Coccia EM (2003) IFN-alpha beta released by Mycobacterium tuberculosis-infected human dendritic cells induces the expression of CXCL10: selective recruitment of NK and activated T cells. J Immunol 170(3):1174–1182

Lash JA, Coates TD, Lafuze J, Baehner RL, Boxer LA (1983) Plasma lactoferrin reflects granulocyte activation in vivo. Blood 61(5):885–888

Lim SY, Raftery M, Cai H, Hsu K, Yan WX, Hseih HL, Watts RN, Richardson D, Thomas S, Perry M, Geczy CL (2008) S-nitrosylated S100A8: novel anti-inflammatory properties. J Immunol 181(8):5627–5636

Lim SY, Raftery MJ, Goyette J, Hsu K, Geczy CL (2009) Oxidative modifications of S100 proteins: functional regulation by redox. J Leukoc Biol 86(3):577–587. doi:10.1189/jlb.1008608

Megjugorac NJ, Young HA, Amrute SB, Olshalsky SL, Fitzgerald-Bocarsly P (2004) Virally stimulated plasmacytoid dendritic cells produce chemokines and induce migration of T and NK cells. J Leukoc Biol 75(3):504–514. doi:10.1189/jlb.0603291

Mozzanica N, Cattaneo A, Boneschi V, Brambilla L, Melotti E, Finzi AF (1990) Immunohistological evaluation of basal cell carcinoma immunoinfiltrate during intralesional treatment with alpha 2-interferon. Arch Dermatol Res 282(5):311–317

Newton RA, Hogg N (1998) The human S100 protein MRP-14 is a novel activator of the beta 2 integrin Mac-1 on neutrophils. J Immunol 160(3):1427–1435

Queen MM, Ryan RE, Holzer RG, Keller-Peck CR, Jorcyk CL (2005) Breast cancer cells stimulate neutrophils to produce oncostatin M: potential implications for tumor progression. Cancer Res 65(19):8896–8904. doi:10.1158/0008-5472.CAN-05-1734

Roth J, Vogl T, Sunderkotter C, Sorg C (2003) Chemotactic activity of S100A8 and S100A9. J Immunol 171(11):5651

Ryckman C, McColl SR, Vandal K, de Medicis R, Lussier A, Poubelle PE, Tessier PA (2003) Role of S100A8 and S100A9 in neutrophil recruitment in response to monosodium urate monohydrate crystals in the air-pouch model of acute gouty arthritis. Arthritis Rheum 48(8):2310–2320. doi:10.1002/art.11079

Schnekenburger J, Schick V, Kruger B, Manitz MP, Sorg C, Nacken W, Kerkhoff C, Kahlert A, Mayerle J, Domschke W, Lerch MM (2008) The calcium binding protein S100A9 is essential for pancreatic leukocyte infiltration and induces

disruption of cell–cell contacts. J Cell Physiol 216(2):558–567. doi:10.1002/jcp.21433

Simard JC, Girard D, Tessier PA (2010) Induction of neutrophil degranulation by S100A9 via a MAPK-dependent mechanism. J Leukoc Biol 87(5):905–914. doi:10.1189/jlb.1009676

Simard JC, Simon MM, Tessier PA, Girard D (2011) Damage-associated molecular pattern S100A9 increases bactericidal activity of human neutrophils by enhancing phagocytosis. J Immunol 186(6):3622–3631. doi:10.4049/jimmunol.1002956

Sroussi HY, Berline J, Dazin P, Green P, Palefsky JM (2006) S100A8 triggers oxidation-sensitive repulsion of neutrophils. J Dent Res 85(9):829–833

Tsuda H, Kozu T, Iinuma G, Ohashi Y, Saito Y, Saito D, Akasu T, Alexander DB, Futakuchi M,Fukamachi K, Xu J, Kakizoe T, Iigo M (2010) Cancer prevention by bovine lactoferrin: from animal studies to human trial. Biometals 23:399–409. doi:10.1007/s10534-010-9331-3

van den Tol MP, ten Raa S, van Grevenstein WM, van Rossen ME, Jeekel J, van Eijck CH (2007) The post-surgical inflammatory response provokes enhanced tumour recurrence: a crucial role for neutrophils. Digit Surg 24(5):388–394. doi:10.1159/000107781

van der Strate BW, Harmsen MC, The TH, Sprenger HG, de Vries H, Eikelboom MC, Kuipers ME, Meijer DK, Swart PJ (1999) Plasma lactoferrin levels are decreased in end-stage AIDS patients. Viral Immunol 12(3):197–203

Vandal K, Rouleau P, Boivin A, Ryckman C, Talbot M, Tessier PA (2003) Blockade of S100A8 and S100A9 suppresses neutrophil migration in response to lipopolysaccharide. J Immunol 171(5):2602–2609

Wada Y, Yoshida K, Tsutani Y, Shigematsu H, Oeda M, Sanada Y, Suzuki T, Mizuiri H, Hamai Y, Tanabe K, Ukon K, Hihara J (2007) Neutrophil elastase induces cell proliferation and migration by the release of TGF-alpha, PDGF and VEGF in esophageal cell lines. Oncol Rep 17(1):161–167

Wislez M, Antoine M, Rabbe N, Gounant V, Poulot V, Lavole A, Fleury-Feith J, Cadranel J (2007) Neutrophils promote aerogenous spread of lung adenocarcinoma with bronchioloalveolar carcinoma features. Clin Cancer Res 13(12):3518–3527. doi:10.1158/1078-0432.CCR-06-2558

Zhao J, Endoh I, Hsu K, Tedla N, Endoh Y, Geczy CL (2011) S100A8 modulates mast cell function and suppresses eosinophil migration in acute asthma. Antioxid Redox Signal 14(9):1589–1600. doi:10.1089/ars.2010.3583

Arch Toxicol (2014) 88:65–75
DOI 10.1007/s00204-013-1086-5

INORGANIC COMPOUNDS

Nanosized zinc oxide particles do not promote DHPN-induced lung carcinogenesis but cause reversible epithelial hyperplasia of terminal bronchioles

Jiegou Xu · Mitsuru Futakuchi · David B. Alexander · Katsumi Fukamachi · Takamasa Numano · Masumi Suzui · Hideo Shimizu · Toyonori Omori · Jun Kanno · Akihiko Hirose · Hiroyuki Tsuda

Received: 25 February 2013 / Accepted: 20 June 2013 / Published online: 6 July 2013

Abstract Zinc oxide (ZnO) is known to induce lung toxicity, including terminal bronchiolar epithelial hyperplasia, which gives rise to concerns that nanosized ZnO (nZnO) might lead to lung carcinogenesis. We studied the tumor promoting activity of nZnO by an initiation–promotion protocol using human c-Ha-*ras* proto-oncogene transgenic rats (H*ras*128 rats). The rats were given 0.2 % N-nitrosobis(2-hydroxypropyl)amine (DHPN) in the drinking water for 2 weeks and then treated with 0.5 ml of 250 or 500 μg/ml nZnO suspension by intra-pulmonary spraying once every 2 weeks for a total of 7 times. Treatment with nZnO particles did not promote DHPN-induced lung carcinogenesis. However, nZnO dose-dependently caused epithelial hyperplasia of terminal bronchioles (EHTB) and fibrosis-associated interstitial pneumonitis (FAIP) that were independent of DHPN treatment. Tracing the fate of EHTB lesions in wild-type rats indicated that the hyperplastic lesions almost completely disappeared within 12 weeks after the last nZnO treatment. Since nZnO particles were not found in the lung and $ZnCl_2$ solution induced similar lung lesions and gene expression profiles, the observed lesions were most likely caused by dissolved Zn^{2+}. In summary, nZnO did not promote carcinogenesis in the lung and induced EHTB and FAIP lesions that regressed rapidly, probably due to clearance of surplus Zn^{2+} from the lung.

Keywords Nanosized zinc oxide particles · Lung toxicity · Lung carcinogenesis · Epithelial hyperplasia of terminal bronchioles · Interstitial pneumonitis · Lung fibrosis

Electronic supplementary material The online version of this article (doi:10.1007/s00204-013-1086-5) contains supplementary material, which is available to authorized users.

J. Xu · D. B. Alexander · H. Tsuda (✉)
Laboratory of Nanotoxicology Project, Nagoya City University, 3-1 Tanabedohri Mizuho-ku, Nagoya 467-8603, Japan
e-mail: htsuda@phar.nagoya-cu.ac.jp

J. Xu · M. Futakuchi · K. Fukamachi · T. Numano · M. Suzui
Department of Molecular Toxicology, Nagoya City University Graduate School of Medical Sciences, 1-Kawasumi, Mizuho-cho, Mizuho-ku, Nagoya 467-8601, Japan

H. Shimizu
Core Laboratory, Nagoya City University Graduate School of Medical Sciences, 1-Kawasumi, Mizuho-cho, Mizuho-ku, Nagoya 467-8601, Japan

T. Omori
Department of Health Care Policy and Management, Nagoya City University Graduate School of Medical Sciences, 1-Kawasumi, Mizuho-cho, Mizuho-ku, Nagoya 467-8601, Japan

J. Kanno · A. Hirose
National Institute of Health Sciences, 1-18-1 Kamiyoga, Setagaya-ku, Tokyo 158-8501, Japan

Introduction

One of the most widely used nanomaterials is nZnO. The worldwide production of nZnO powder is increasing every year and was reported to have reached 1.4 million tons in 2011. It is used in rubber industry and electronics and in commercial products such as sunscreens and paints. In the biomedical field, it is used in baby powders, antiseptic ointments, and zinc oxide tapes to treat a variety of skin conditions (Baldwin et al. 2001; Hughes and McLean 1988). Recently, nZnO has gained interest in cancer applications or as an active anticancer drug (Rasmussen et al. 2010).

Micron or larger-sized ZnO particles are considered to be "Generally Recognized as Safe" (GRAS) in food

additives by the FDA. However, exposure to fumes containing ZnO and other metal particles during welding or galvanizing processes is known to lead to metal fume fever (Antonini et al. 2003; Drinker and Fairhall 1933; Fine et al. 1997). Recent reports have shown that nZnO affects cell viability and induces reactive oxygen species (ROS) in many mammary cell types in tissue culture (Deng et al. 2009; Lee et al. 2008; Xia et al. 2008; Yang et al. 2009), cause proliferation of airway epithelial cells, goblet cell hyperplasia, interstitial pulmonary inflammation and fibrosis (Cho et al. 2011), and reversible inflammatory reaction in the bronchoalveolar lavage fluid in animal studies (Sayes et al. 2007; Warheit et al. 2009). nZnO also leads to DNA damage (Kermanizadeh et al. 2012) and micronuclei formation in vitro (Valdiglesias et al. 2013). While these in vitro and in vivo studies have provided some information on acute toxic effects of nZnO on certain cell types and animals, further in vivo studies are needed to determine whether nZnO has chronic toxic effects as in some other metal oxide particles. For example, epidemiological data indicate that exposures of aluminum oxide or iron oxide lead to pneumoconiosis in human (Hull and Abraham 2002; Sano 1963); titanium dioxide has carcinogenic activity in the rat lung (Heinrich et al. 1995; Xu et al. 2010). Such chronic toxicity data will have more impact on risk assessment of nZnO.

Since nZnO induces inflammatory reaction, ROS production, and genotoxicity, which are implicated in cancer development, in the present study, we tested the lung carcinogenicity of nZnO by an initiation–promotion protocol using human c-Ha-*ras* proto-oncogene transgenic (H*ras* 128) rats, which have the same susceptibility to chemically induced lung carcinogenesis as their parent wild-type rats, but are highly susceptible to mammary tumor induction (Tsuda et al. 2005). The results indicated that nZnO did not have promotion effect on DHPN-induced lung and mammary carcinogenesis and caused reversible EHTB and FAIP.

Materials and methods

Animals

Forty-three female transgenic rats carrying the human c-Ha-RAS proto-oncogene (H*ras*128 rats) and 42 female wild-type Sprague–Dawley rats were obtained from CLEA Japan Co., Ltd. (Tokyo, Japan). The animals were housed in the Animal Center of Nagoya City University Medical School and maintained on a 12-h light/12-h dark cycle and received Oriental MF basal diet (Oriental Yeast Co. Ltd., Tokyo, Japan) and water ad libitum. The study was conducted according to the Guidelines for the Care and Use of Laboratory Animals of Nagoya City University Medical School, and the experimental protocol was approved by the Institutional Animal Care and Use Committee (H22M-19).

Preparation, characterization of nZnO suspensions, and administration of nZnO to the lung

Zinc oxide particles (CAS No. 1314-13-2, MZ-500, without coating, with a mean primary diameter of 25 nm) were obtained from Tayca Cooperation, Osaka, Japan. The particles were suspended in 0.1 % Tween 20 saline at 250 or 500 μg/ml. The suspension was sonicated for 20 min to prevent aggregate formation.

Characterization of nZnO was conducted as follows: the shape of nZnO in the suspensions was imaged by transmission electron microscopy (TEM); element analysis was performed by an X-ray microanalyzer (EDAX, Tokyo, Japan), after aliquots of nZnO were loaded on a carbon sheet; the size distribution of nZnO in the 500 μg/ml suspension was analyzed using a Particle Size Distribution Analyzer (Shimadzu Techno-Research, Inc., Kyoto, Japan). The characterization results are shown in Figure S1.

Before being administrated to rats, the nZnO suspensions were further sonicated for 20 min. 0.5 ml of the nZnO suspensions was administrated to the lung by intra-pulmonary spraying (IPS) as described previously (Xu et al. 2010).

Carcinogenicity study

The carcinogenic activity of nZnO was assessed in female H*ras*128 rats using an initiation–promotion protocol by which we used previously to evaluate lung and mammary carcinogenicity of titanium dioxide nanoparticles (Xu et al. 2010). Briefly, three groups of 10–11 female H*ras*128 rats aged 6 weeks were given 0.2 % DHPN (Wako Chemicals, Co., Ltd. Osaka, Japan) in the drinking water for 2 weeks, and Groups 4 and 5 (6 rats each) were given drinking water without DHPN. Two weeks later, Group 1 and Group 4 were administered 0.1 % Tween 20 saline, and Group 2, Group 3, and Group 5 were administered 250, 500, and 500 μg/ml nZnO suspensions by IPS once every two weeks from the end of week 4 to week 16, a total of 7 times. The total amounts of nZnO administered to Groups 1, 2, 3, 4, and 5 were 0, 0.875, 1.75, 0, and 1.75 mg/rat, respectively. The dosing was determined according to the permissible exposure limit for zinc oxide particles of the Occupational Safety and Health Administration (OSHA) (see Discussion). Three days after the last treatment, animals were killed and the organs (brain, lung, liver, spleen, kidney, mammary gland, ovaries, uterus, and neck lymph nodes) were fixed in 4 % paraformaldehyde in PBS buffer adjusted to pH 7.3 and processed for histological examination and transmission electron microscopy (TEM).

Light microscopy, polarized light microscopy, and transmission electron microscopy

Hematoxylin–Eosin (H&E)-stained pathological slides of the lung and other major organs were used to observe nZnO with a light microscope and polarized light microscope (PLM) (Olympus BX51N-31P-O polarized light microscope, Tokyo, Japan) at 1,000× magnification. Localization of the illuminated particles was confirmed in the same H&E-stained sections after removing the polarizing filter.

Paraffin blocks were deparaffinized and embedded in epon resin and processed for nZnO observation and zinc element analysis, using a JEM-1010 transmission electron microscope (TEM) (JEOL, Co. Ltd, Tokyo, Japan) equipped with an X-ray microanalyzer (EDAX, Tokyo, Japan).

Immunohistochemistry and Azan–Mallory staining

PCNA was detected using an anti-PCNA monoclonal antibody (Clone PC10, Dako Japan Inc., Tokyo, Japan). The antibody was diluted 1:200 in blocking solution and applied to deparaffinized slides, and the slides were incubated at 4 °C overnight. The slides were then incubated for 1 h with biotinylated species-specific secondary antibodies diluted 1:500 (Vector Laboratories, Burlingame, CA) and visualized using avidin-conjugated horseradish peroxidase complex (ABC kit, Vector Laboratories). To assess lung fibrosis, paraffin-embedded slides were deparaffinized, and collagen fibers were visualized by Azan–Mallory staining.

Reversibility study and effects of $ZnCl_2$ solution

To assess whether nZnO-induced terminal bronchiolar epithelial hyperplasia, interstitial pneumonitis, and lung fibrosis are reversible, we conducted reversibility experiments. Seven groups of 5 female wild-type Sprague–Dawley rats aged 10 weeks were administrated 0.5 ml of 0.1 % Tween 20 saline or 500 μg/ml nZnO suspension by IPS 2 times per week for 4 weeks. Group 1 was treated with 0.1 % Tween 20 saline and killed 1 day after the last IPS. Groups 2–7 were treated with 0.5 ml of 500 μg/ml nZnO suspension and killed at 1 day and 2, 4, 6, 8, and 12 weeks after the last IPS. For the comparison of the effects of zinc ion and nZnO, Group 8 was treated with 0.5 ml of 6.17 mM $ZnCl_2$ solution (the molecular amount is equal to that of 500 μg/ml nZnO suspension) by IPS at the same frequency and time period as the nZnO groups and killed 1 day after the last IPS. The left lung was cut into pieces and frozen in liquid nitrogen for biochemical analysis, and the right lung was processed for histological examination. Other major organs were excised for histological examination, and the blood was collected for cytological and biochemical analysis.

Gene expression analysis

The left lungs from Groups 1, 2, and 8 in the reversibility study described above were used for isolation of RNA. RNA was isolated by using TRizol reagent (Invitrogen of Life Technologies, CA).

For microarray analysis, 1 μg RNA from each rat of Group 1 was combined and 1 μg RNA from each rat of Group 2 was combined. The quality of the 2 mixtures of RNA samples was assessed and quantified using the Agilent 2100 BioAnalyzer RNA Nano chip system (Agilent Technologies, CA) prior to further manipulation. Microarray analysis was conducted by the 3-D Gene Chip (Toray Industries Inc., Kanagawa, Japan), and a total of 20,000 genes were analyzed. Microarray-based pathway analysis was performed by Toray Industries Inc., Kanagawa, Japan.

For reverse transcription-PCR (RT-PCR) and real-time PCR, first-strand cDNA synthesis from 1 μg of RNA was performed using SuperScript™ III First-Strand Synthesis System (Invitrogen of Life Technologies, CA) according to the manufacturer's instructions. Primers are as follows: forward primer, 5′-TAGAATCGAGGTGCACAGGAGT-3′, reverse primer, 5′-TATTCCAGCAGGCTGTCAAAGA-3′, product size, 228 bp for Orm1; forward primer, 5′-AAGTGGAGGAGCAGCTGGAGTGG-3′, reverse primer, 5′-CCAAAGTAGACCTGCCCGGACTC-3′, product size, 155 bp for Tnfa, and forward primer, 5′-AGCCATGTACGTAGCCATCC-3′, reverse primer, 5′-CTCTCAGCTGTGGTGGTGAA-3′, product size, 228 bp for Actb. RT-PCR was conducted using an iCycler (BioRad Life Sciences, CA) as follows: 95 °C 20 s, 60 °C 20 s, 72 °C 30 s, 30 cycles for Orm1; 95 °C 20 s, 60 °C 20 s, 72 °C 20 s, 25 cycles for Tnfa, and 95 °C 20 s, 60 °C 20 s, 72 °C 30 s, 15 cycles for Actb. Real-time PCR analysis of Orm1 and Tnfa gene expression was performed with the 7300 real-time PCR system (Applied Biosystem, CA) using the premix reagent Power SYBR Green PCR Master Mix (Applied Biosystem, CA) according to the manufacturer's instructions. The Actb gene was used as the normalizing reference gene.

Determination of zinc ion

For detection of Zn^{2+} content in the lung tissue, 50–100 mg of the frozen lung tissues from the reversibility study described above were thawed at room temperature, rinsed with cold PBS 3 times, and homogenized for 30 s at the highest speed in 1 ml of T-PER, tissue protein extraction reagent (Pierce, Rockford, IL), with Polytron R PT 2100 homogenizer (Capitol Scientific Inc., TX). The homogenates were clarified by centrifugation at 10,000×g for 15 min at 4 °C, and the supernatants were used for Zn^{2+}

detection. Zn^{2+} detection was performed using QuantiChrom™ Zinc Assay kit (BioAssay Systems, CA) according to the manufacturer's instructions.

In vitro nZnO dissolution assay

5 μl of 500 μg/ml nZnO suspension (2.5 μg/tube) and increasing amounts of 1 mg/ml human α 1 acid glycoprotein (Sigma-Aldrich, product number G9885) or bovine serum albumin (Sigma-Aldrich, product number A2058) were added to microtubes, and the total volume of each tube was adjusted to 100 μl with 0.1 % Tween 20 saline. The final protein concentration of human α 1 acid glycoprotein or bovine serum albumin was 0, 100, 200, 300, 400, and 500 μg/ml. The tubes were then incubated at 37 °C for 2 h. The nZnO particles were removed by centrifugation at 10,000×*g* for 5 min, and Zn^{2+} concentration in the supernatants was determined as described above.

In vitro cytotoxicity assay

The induction and preparation of rat primary alveolar macrophages (PAM) has been described (Xu et al. 2010). 5×10^3 PAMs, 1×10^3 A549 cells (human lung adenocarcinoma cell line), and 2×10^3 CCD34 cells (human lung fibroblast cell line) were seeded into 96-well culture plates and cultured overnight in 100 ml of RPMI 1,640 containing 10 % FBS. The cells were added with nZnO suspension or ZnCl2 solution to final concentrations of 0, 1, 5, or 25 μg/ml of nZnO and 0, 12.3, 61.7, or 308.6 nM of ZnCl2 (1, 5, and 25 μg/ml of nZnO are equal to 12.3, 61.7, and 308.6 nM of ZnCl2, respectively, in the amount of zinc element) and incubated for another 72 h. The cell viability was then determined using the Cell Counting Kit-8 (Dojindo Molecular Technologies, Rockville, MD) according to the manufacturer's instruction.

Statistical analysis

Statistical analysis was performed using ANOVA. Statistical significance was analyzed using a two-tailed Student's *t*-test. A p value of <0.05 was considered to be significant.

Results

Carcinogenesis study in H*ras*128 rats

DHPN-induced lung alveolar cell hyperplasia and adenoma development was used for the end point observation to assess the carcinogenicity of nZnO in our medium-term assay. As shown in Table 1, the incidence and multiplicity (number/cm^2 lung tissue section) of

Table 1 Effect of nZnO on lung proliferative lesions in H128-*ras* rats

Treatment	No. of rats	DHPN-induced proliferative lesions						DHPN-independent EHTB[a]	
		ACH[a]		Ade[a]		ACH + Ade		Inc. (%)	Multiplicity[b] (no./cm^2 lung)
		Inc.[a] (%)	Multiplicity[b] (no./cm^2 lung)	Inc. (%)	Multiplicity[b] (no./cm^2 lung)	Inc. (%)	Multiplicity[b] (no./cm^2 lung)		
DHPN + vehicle	11	11 (100)	2.43 ± 1.29	2 (18.1)	0.09 ± 0.20	11 (100)	2.52 ± 1.26	0 (0)	0
DHPN + 250 μg/ml nZnO	10	10 (100)	1.64 ± 1.09	3 (30.0)	0.12 ± 0.19	10 (100)	1.76 ± 1.03	7 (70)	0.86 ± 0.86 **
DHPN + 500 μg/ml nZnO	10	10 (100)	1.83 ± 1.05	5 (50.0)	0.30 ± 0.31	10 (100)	2.13 ± 1.23	10 (100)	4.93 ± 1.95 ***
Vehicle	6	0	0	0	0	0	0	0	0
500 μg/ml nZnO	6	2 (33.3)	0.16 ± 0.26	0	0	2 (33.3)	0.16 ± 0.26	6 (100)	3.91 ± 1.29 ***

[a] ACH, Ade, EHTB, and Inc. are abbreviations for alveolar cell hyperplasia, adenoma, epithelial hyperplasia of terminal bronchioles, and incidence, respectively

[b] Multiplicity is expressed as mean ± s.d

** and *** represent p values <0.01 and 0.001, respectively, versus DHPN + vehicle or vehicle

alveolar cell hyperplasia and adenoma in the groups treated with nZnO were not significantly different from the DHPN alone group. In the rats which received nZnO treatment without prior DHPN treatment, alveolar cell proliferation foci, recognized as thickening of the alveolar wall with proliferative alveolar epithelium, were observed, but significant differences from the saline group were not observed. In the mammary gland, significant inter-group difference in incidence and multiplicity of mammary tumors was also not observed (data not shown).

A notable lesion induced in all the nZnO-treated groups was epithelial hyperplasia of terminal bronchioles (EHTB). The EHTB lesions had increased cell density, often with the epithelial cells arranged in 1–3 layers, and partly extended bronchiolar structures with transition to the normal

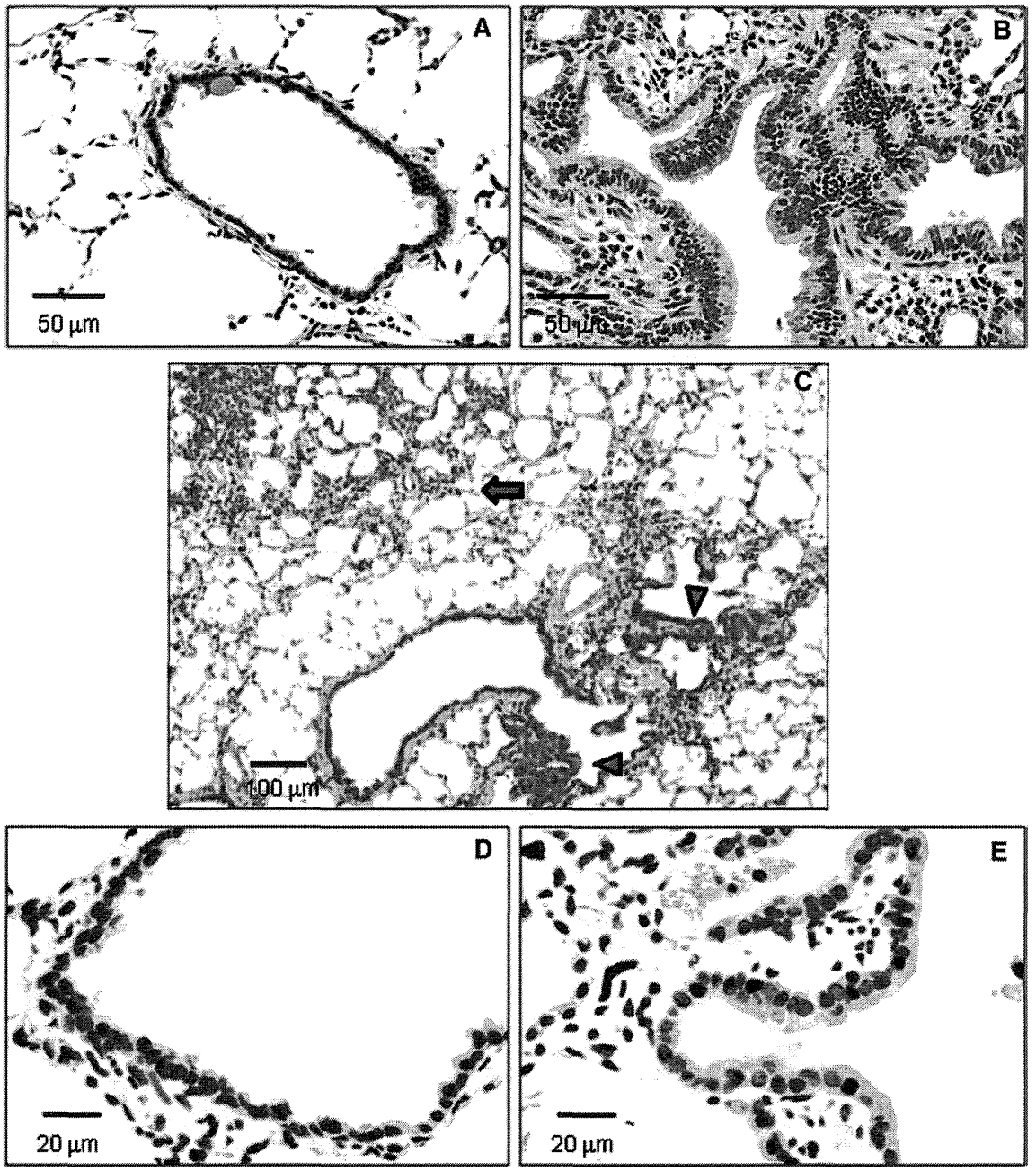

Fig. 1 Induction of EHTB by nZnO. **a** representative normal terminal bronchiolar epithelium (NTBE); **b** EHTB in H&E-stained slides; **c** images and localizations of DHPN-induced alveolar hyperplasia (*arrow*) and nZnO-induced EHTB (*arrow heads*); **d** images of PCNA immunostaining in NTBE; and **e** in EHTB

terminal bronchioles (Fig. 1a, b). The EHTB lesions were independently localized from the DHPN-induced alveolar cell hyperplastic lesions (Fig. 1c). The incidences and multiplicity (number/cm^2 lung tissue section) of EHTB in the groups treated with nZnO were significantly increased compared with that of the DHPN alone group. The increase was dose-dependent (Spearman rank correlation test, $p < 0.001$) (Table 1). Immunostaining with proliferating cell nuclear antigen (PCNA) indicated that proliferating bronchiolar epithelial cells were preferentially found in the EHTB lesions, but rarely found in the normal terminal bronchial epithelial areas (Fig. 1d, e).

Another lesion found in the groups treated with nZnO, and also independent of DHPN treatment, was interstitial pneumonitis (Fig. 2a). The lesion was usually associated with fibrosis of various thicknesses of the septal wall extruding into the alveolar structure (blue staining in Fig. 2b). Quantitative analysis indicated a significant increase in the fibrotic area in the rats treated with nZnO compared with that of rats treated with DHPN alone (Fig. 2c), and the increase was dose-dependent (Spearman rank correlation test, $p < 0.001$). In addition, the EHTB lesions often occurred near or within interstitial pneumonitis areas.

Light microscopic observation of the alveoli of the rats treated with nZnO showed infiltration of numerous macrophages mixed with a few neutrophils, eosinophils, and lymphocytes (data not shown). The nZnO particles were not found in any of the alveolar macrophages; these macrophages contained numerous vacuolar vesicles in the cytoplasm (Fig. 2d). Transmission electron microscopic (TEM) observation showed that nZnO particles were not found within the vacuolar vesicles (Fig. 2e) or in any alveolar tissue cells (Fig. 2f). The absence of a zinc peak was confirmed by elemental scanning with TEM-X-ray microanalysis (Figure S2). nZnO particles were also not detected under polarized light microscope observation. This feature was in contrast with titanium dioxide nanoparticles which were clearly observed in alveolar macrophages (Figure S3).

Reversibility of EHTB and FAIP in wild-type rats

As in the H*ras*128 transgenic rats, nZnO induced EHTB and FAIP in wild-type Sprague–Dawley (SD) rats (Fig. 3a), and nZnO was not found in the lung tissue. nZnO-induced EHTB and FAIP gradually regressed with time (Fig. 3a), and the number of EHTB foci per square centimeter lung tissue section decreased from 9.81 ± 1.42 at day 1 to 0.06 ± 0.13 at week 12 after cessation of nZnO exposure (Fig. 3b). The total Zn^{2+} content in the lung tissue also gradually decreased (Fig. 3c) and was positively correlated with the number of EHTB ($r = 0.96$ by Pearson correlation test).

Microarray analysis

Microarray analysis of the lung tissue indicated that nZnO treatment up-regulated the expression of 738 genes and down-regulated the expression of 267 genes (data not shown). The up-regulated inflammation-associated genes included chemotactic chemokines such as Cxcl5, Cxcl11, Ccl7, Cxcl2, Ccl2, and Cxcl1, proinflammatory cytokines such as Tnfa and Il6, and the acute-phase reactant Orm1 (Table S1). Pathway analysis showed an increase in inflammatory responses in which macrophages and TNFα play a central role (Figure S4). The gene expression profiling was consistent with the strong inflammatory responses in the lung observed by histological examination. Other pathways up-regulated by nZnO included classical complement activation pathway, matrix metalloproteinase pathway, cholesterol biosynthesis pathway and striated muscle contraction pathway, and treatment of nZnO down-regulated the adipogenesis pathway (data not shown).

Effects of $ZnCl_2$ solution on the lung of wild-type rats

To check whether the nZnO-induced EHTB and FAIP were due to dissolution of nZnO to Zn^{2+}, we administered $ZnCl_2$ solution (the molecular amount is equal to that of 500 μg/ml nZnO suspension) to the lung of rats by IPS. The lesions were histologically similar to those observed in the nZnO-treated rats (Fig. 4a, b, c). Quantitative analysis of EHTB indicated that the number of EHTB induced by $ZnCl_2$ solution and nZnO was comparable (Fig. 4d).

To examine whether Zn^{2+} and nZnO have the same underlying molecular mechanisms, two genes, Tnfa and Orm1, which were determined to be up-regulated in the nZnO-treated rats by microarray analysis, were chosen for gene expression analysis. These genes were chosen because Tnfa-encoded tumor necrosis factor alpha is a multifunctional proinflammatory cytokine involved in a variety of acute and chronic inflammatory responses, and Orm1-encoded alpha 1 acid glycoprotein (AGP) is an acute-phase protein usually synthesized by hepatocytes in response to trauma, infection, and inflammation (Fournier et al. 2000). RT-PCR (Fig. 4e) and real-time PCR (Fig. 4f) showed that treatment with both $ZnCl_2$ solution and nZnO increased the expression of Tnfa and Orm1 genes in the lung tissue, with a little higher induction in the $ZnCl_2$ solution treated rats. Similarly, increased expression of Orm1 genes was found in primary alveolar macrophages exposed to nZnO in vitro (Fig. 4g). Interestingly, addition of human AGP to nZnO suspension dose-dependently promoted dissolution of nZnO from 59.1 nmol/ml (19.7 % dissolved,

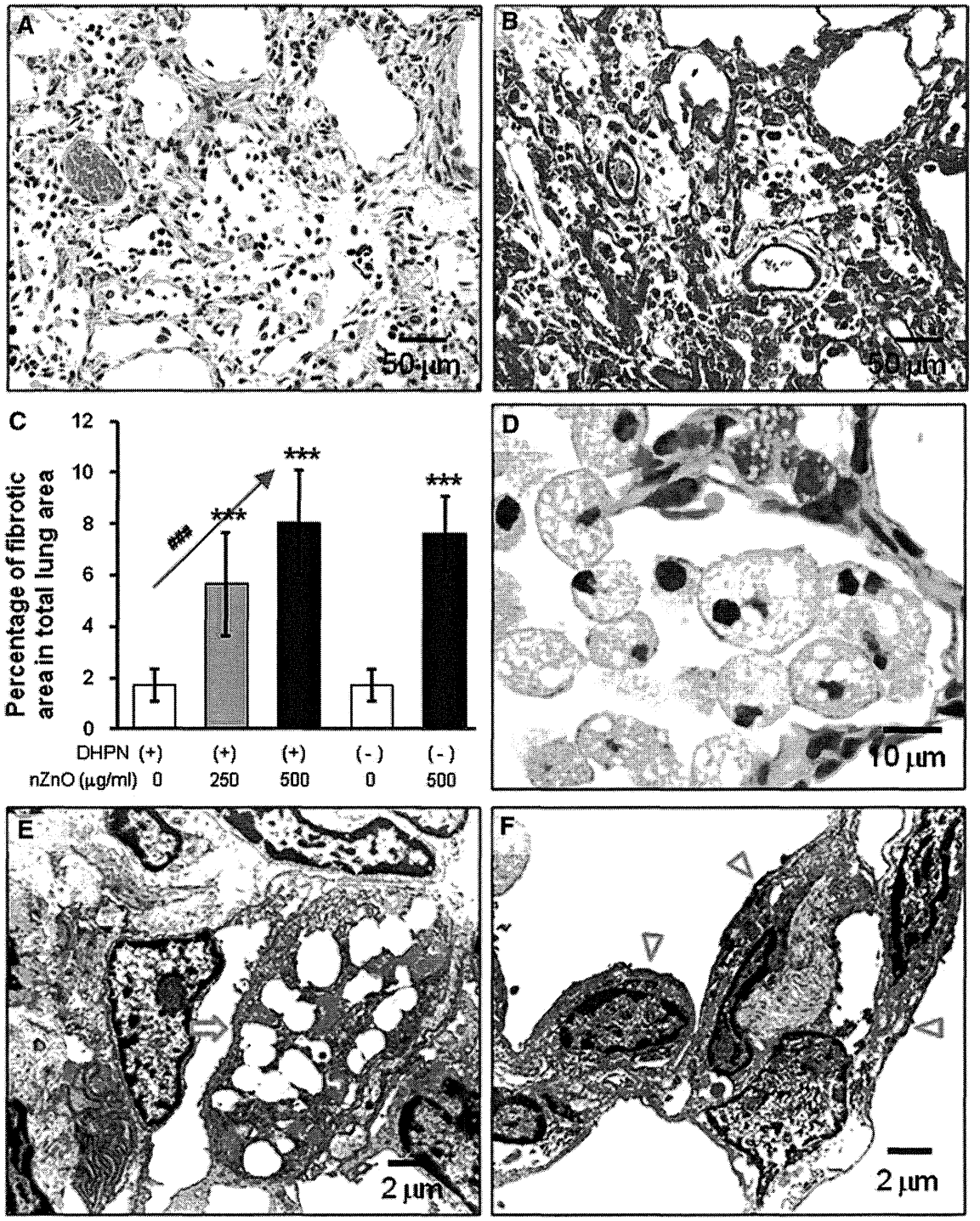

Fig. 2 Induction of FAIP and observation of nZnO particles. **a** representative image of FAIP in rats treated with nZnO; **b** image of Azan–Mallory staining in the lung of rats treated with nZnO, showing collagen fibers; **c** percentage of the fibrotic area in total lung tissue area. ***<0.001 by two-tailed Student's *t*-test versus the vehicle group; and ###$p < 0.001$ by Spearman rank correlation test. **d** image showing alveolar macrophages with vacuous phagocytosis vesicles; **e** and **f** TEM images showing alveolar macrophages (*arrow*) and epithelium (*arrow heads*), no nZnO particles being observed

without addition of AGP) to 117.3 nmol/ml (39.1 % dissolved after addition of 500 µg/ml of AGP), while addition of bovine serum albumin (BSA) had little effect on dissolution of nZnO (Fig. 4h). Exposure of both nZnO and $ZnCl_2$ solution resulted in dose-dependent cell death in vitro (Figure S5).

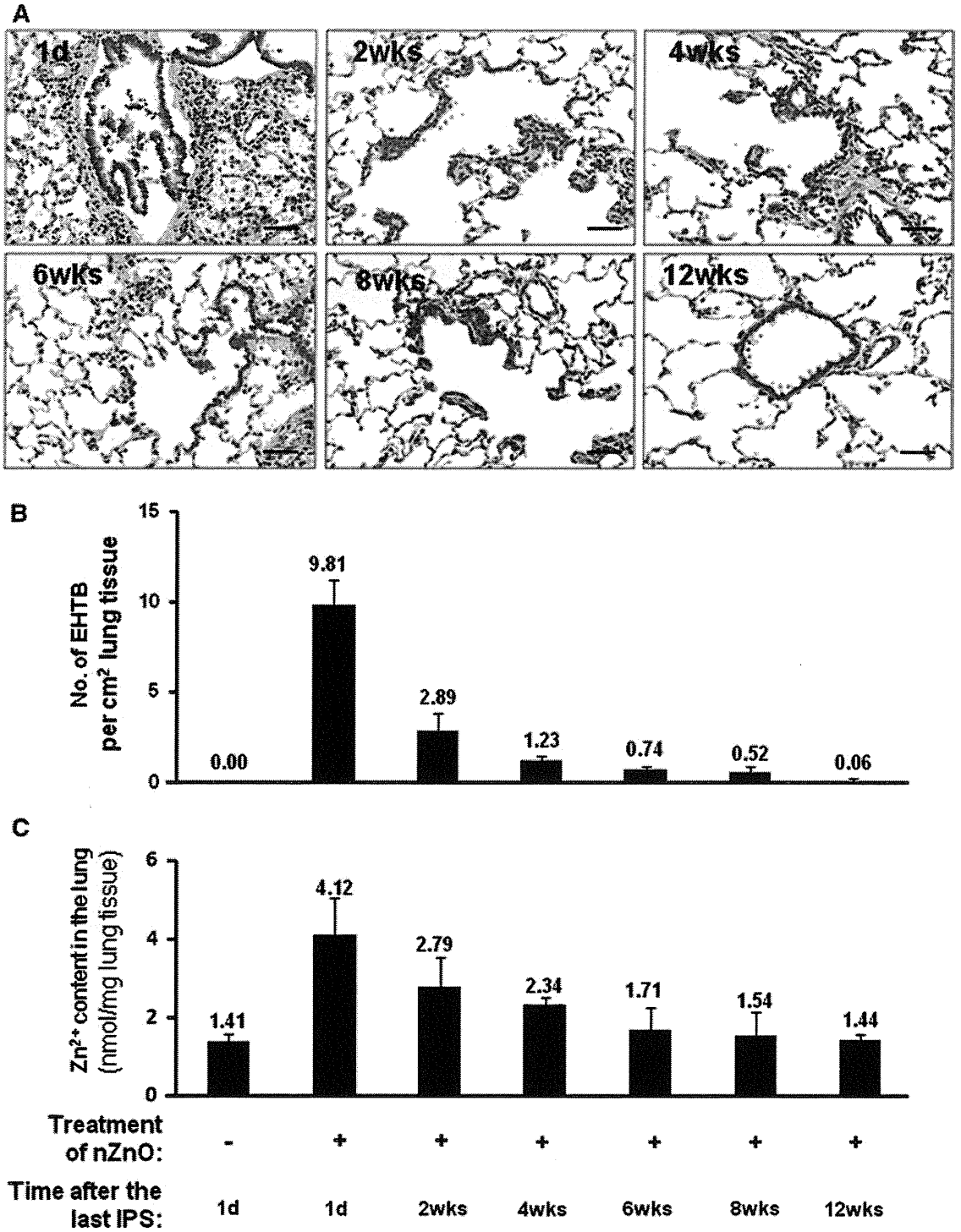

Fig. 3 nZnO-induced EHTB and FAIP are reversible. Wild-type rats were treated with 500 μg/ml nZnO by IPS 2 times/week for 4 weeks and killed at different time points of 1 day (1d) and 2, 4, 6, 8, and 12 weeks (wks) after the last IPS. **a** histological images of the lung tissues; **b** number of EHTB per cm^2 lung tissue and **c** Zn^{2+} content in the lung tissues at different time points. *Bars* = 50 μm

Effects of nZnO particles and $ZnCl_2$ solution on other organs and serum of wild-type rats

Obvious lesions and macrophages containing vacuolar vesicles were not found in other major organs including the liver, kidney, spleen, or brain by histological examination (data not shown). The results of blood cell examination are shown in Table S2: The only changes were increased proportions of monocytes and eosinophils that were rapidly recovered within 2 weeks post exposure. Biochemical

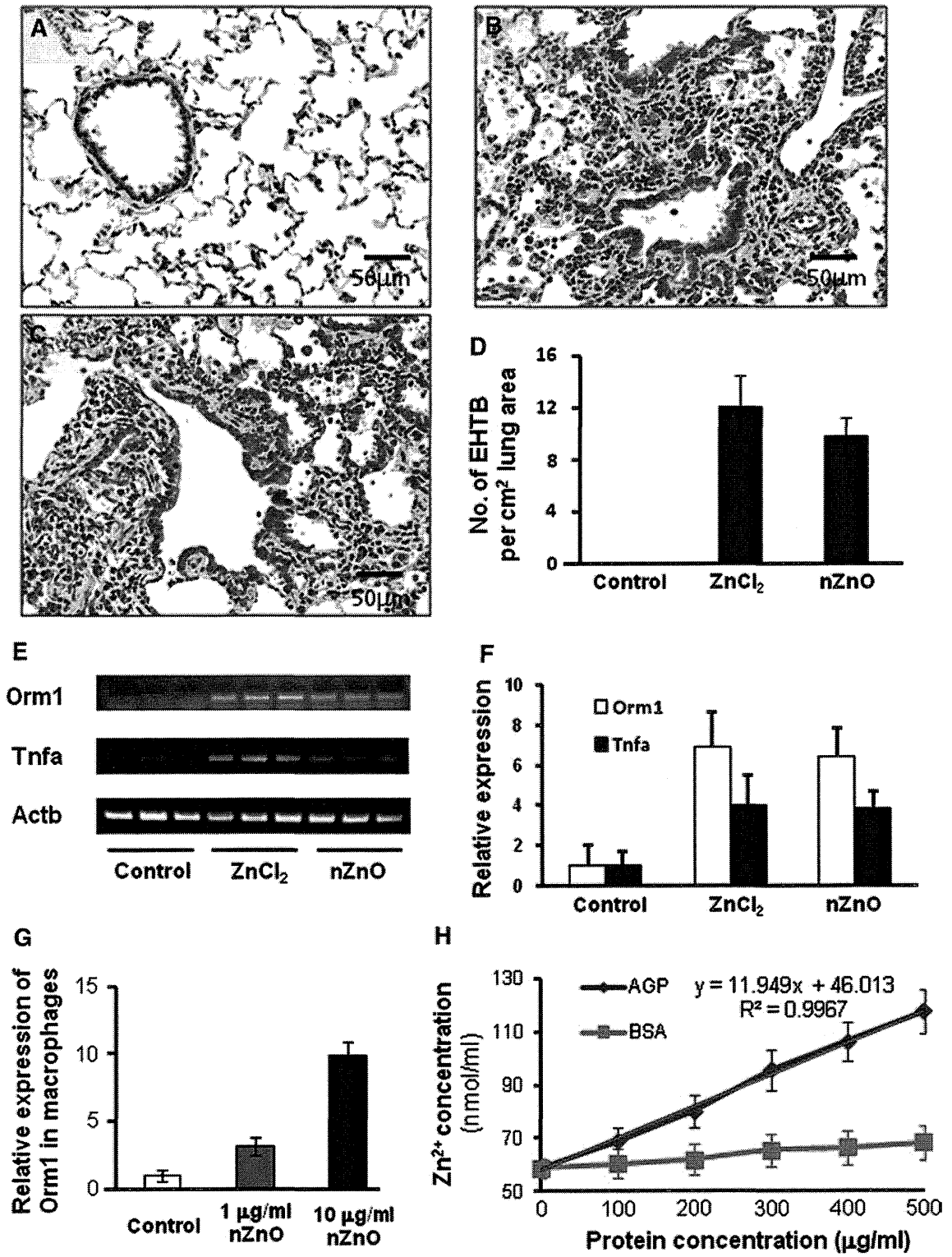

Fig. 4 Similar effects of $ZnCl_2$ solution and nZnO in induction of EHTB and FAIP in wild-type rats. **a** H&E-stained slides of the lungs of rats treated with vehicle; **b** with nZnO; and **c** with $ZnCl_2$ solution, showing EHTB and FAIP; **d** comparable number of EHTB per square centimeter of the lung tissues induced by treatment of $ZnCl_2$ and nZnO; **e** gene expression determined by RT-PCR of Orm1 and Tnfa, with Actb gene as an internal control; **f** real-time PCR analysis of gene expression of Orm1 and Tnfa, which was normalized with Actb expression; **g** induction of Orm1 expression in primary alveolar macrophages exposed to nZnO; and **h** effect of human alpha 1 acid glycoprotein (AGP) and bovine serum albumin (BSA) on dissolution of nZnO in vitro

examination of serum markers for tissue and organ injuries indicated no significant changes compared to the vehicle group (Table S3). Administration of nZnO or $ZnCl_2$ to the lung led to a transient increase in serum Zn^{2+} concentration which returned to normal levels within 2 weeks after administration. The elevated serum Zn^{2+} did not affect the homeostasis of the other ions examined (Table S4).

Discussion

In vivo nanomaterial toxicity usually implicates oxidative stress, inflammation (Nel et al. 2006), and other biological responses depending on the individual nanomaterial. In vitro assays related to carcinogenicity, such as mammalian cell transformation and gene mutation assays, cannot represent the complex in vivo processes of different biological alterations and are not always suitable for risk assessment of nanomaterial carcinogenicity. In the present study, we tested the carcinogenic activity of nZnO in H*ras*128 rats by an initiation–promotion protocol, by which we previously found promotion effect of nanosized titanium dioxide on DHPN-induced lung and mammary carcinogenesis (Xu et al. 2010). nZnO did not show any promotion effects on lung proliferative or neoplastic lesions, indicating that nZnO is not carcinogenetic. Also, nZnO did not promote DHPN-induced mammary carcinogenesis.

On the other hand, nZnO was found to induce EHTB in H*ras*128 rats and wild-type SD rats. EHTB is a proliferative lesion of the terminal bronchiolar epithelium. It should be noted that the localization of EHTB was independent from that of DHPN-induced alveolar cell hyperplasia. This observation clearly indicates that the DHPN-induced alveolar cell hyperplasia and EHTB have different etiology, the latter being induced by nZnO. We also observed 2 cases of alveolar cell hyperplasia out of 6 cases in the nZnO alone group. This is not significant and thus considered to be spontaneous or an inflammation-associated event. The EHTB lesions regressed when administration of nZnO was discontinued and completely disappeared after 12 weeks. Along with EHTB, the interstitial inflammatory changes often observed surrounding the EHTB lesions also regressed. Our data and other reports (Cho et al. 2011) indicate that the EHTB lesions do not progress directly to cancers but are reactive proliferation associated with inflammatory events. Similar reversible inflammatory changes in the bronchoalveolar lavage fluids by administration of nanoscale or fine ZnO particles via inhalation or intratracheal instillation have previously been reported (Warheit et al. 2009).

nZnO particles were not found in alveolar macrophages, in the lung tissue, or in other organs, suggesting that the particles were dissolved to Zn^{2+}. Accordingly, we conducted experiments to determine whether Zn^{2+} would induce similar lesions. $ZnCl_2$ solution induced closely similar lung lesions and gene expression profiles as nZnO, demonstrating that the observed lung lesions were caused by Zn^{2+}. This was confirmed by increased Zn^{2+} level in the lung and serum after administration of nZnO. Interestingly, treatment with nZnO up-regulated the expression of the Omr1 gene in both the lung and the alveolar macrophages, and in vitro addition of Omr1-encoded AGP dose-dependently promoted nZnO dissolution. After Zn^{2+} was cleared from the lung, the EHTB and FAIP lesions disappeared, and this was evidenced by the positive correlation of EHTB number with Zn^{2+} content in the lung. Dissolution of nZnO has been reported to be particle size- and pH-dependent (Mudunkotuwa et al. 2012). Increased Omr1 expression possibly alters the microenvironment of the alveolar macrophages and the lung which accelerates nZnO dissolution. The elevated Zn^{2+} from nZnO dissolution possibly interferes with zinc ion homeostasis and leads to cytotoxic effects (Kao et al. 2012).

According to OSHA, the permissible exposure limit for zinc oxide particles is 15 mg/m^3 of air for total dust and 5 mg/m^3 for the respirable fraction (http://www.osha.gov/SLTC/healthguidelines/zincoxide/recognition.html). The inhalation exposure limit per kilogram of body weight per day for the respirable fraction is 192 μg, calculated from 6,000 ml of minute respiratory volume and 8 working hours for a 75 kg body weight worker. The dosing in the carcinogenesis study of the present study was approximately 35.5 and 71 μg/kg body weight a day (calculated from 125 to 250 μg every two weeks for a 250 g rat) and is lower than the OSHA limit for humans. Since nZnO has more potential to be ionized than larger ZnO particles because of its higher surface area (Mudunkotuwa et al. 2012), this feature should be taken into regulatory consideration.

It has been estimated that engineered nanomaterials will become a $1 trillion enterprise by 2015 (Nel et al. 2006), and ensuring health and environmental safety is a challenging task to the nanotechnology industry. Among numerous engineered nanomaterials, metal based or carbon based, most of which have been shown to have toxic effects to at least some extent, nZnO is a promising nanomaterial for biomedical applications. The results of the present study indicate that, although nZnO induced reversible lung toxicity, it did not cause carcinogenic or chronic progressive inflammatory lesions. Also, since it is biodegradable to ions, nZnO is easily cleared from the body (Rasmussen et al. 2010). Our study also suggests that the toxic effects of nZnO can be further decreased if efforts such as proper dosing and surface coating are made to lower the Zn^{2+} release from nZnO.

In conclusion, treatment of nZnO by IPS did not promote lung and mammary carcinogenesis in our carcinogenesis model. Although nZnO induced EHTB and FAIP, the lesions regressed rapidly along with clearance of surplus Zn^{2+} from the lung and serum. Thus, from a toxicological viewpoint, under the present experimental conditions, exposure of the lung to nZnO does not cause progressive neoplastic development or chronic fibrosis in the lung. These findings will be helpful in evaluating of the safety of nZnO used in biomedical applications, in which its use is of rather short duration, although long-term studies including inhalation studies are required to assess their occupational and environmental health hazards.

Acknowledgments This work was supported by Health and Labor Sciences Research Grants (Research on Risk of Chemical Substance 21340601, H21-kagaku-ippan-008, H24-kagaku-ippan-009 and H22-kagaku-ippan-005) from the Ministry of Health, Labor and Welfare, Japan. We thank A. Iezaki for her excellent secretarial assistance for the work.

Conflict of interest The authors declare that they have no conflict of interest.

References

Antonini JM, Lewis AB, Roberts JR, Whaley DA (2003) Pulmonary effects of welding fumes: review of worker and experimental animal studies. Am J Ind Med 43:350–360

Baldwin S, Odio MR, Haines SL, O'Connor RJ, Englehart JS, Lane AT (2001) Skin benefits from continuous topical administration of a zinc oxide/petrolatum formulation by a novel disposable diaper. J Eur Acad Dermatol Venereol 15(Suppl 1):5–11

Cho WS, Duffin R, Howie SE, Scotton CJ, Wallace WA, Macnee W, Bradley M, Megson IL, Donaldson K (2011) Progressive severe lung injury by zinc oxide nanoparticles; the role of Zn2+ dissolution inside lysosomes. Part Fibre Toxicol 8:27–43

Deng X, Luan Q, Chen W, Wang Y, Wu M, Zhang H, Jiao Z (2009) Nanosized zinc oxide particles induce neural stem cell apoptosis. Nanotechnology 20:115101

Drinker CK, Fairhall LT (1933) Zinc in relation to general and industrial hygiene. Public Health Rep 48:955–961

Fine JM, Gordon T, Chen LC, Kinney P, Falcone G, Beckett WS (1997) Metal fume fever: characterization of clinical and plasma IL-6 responses in controlled human exposures to zinc oxide fume at and below the threshold limit value. J Occup Environ Med 39:722–726

Fournier T, Medjoubi NN, Porquet D (2000) Alpha-1-acid glycoprotein. Biochim Biophys Acta 1482:157–171

Heinrich U, Fuhst R, Rittinghausen S, Creutzenberg O, Bellmann B, Koch K, Levsen K (1995) Chronic inhalation exposure of wistar rats and two different strains of mice to diesel engine exhaust, carbon black, and titanium dioxide. Inhalation Toxicol 7:533–556

Hughes G, McLean NR (1988) Zinc oxide tape: a useful dressing for the recalcitrant finger-tip and soft-tissue injury. Arch Emerg Med 5:223–227

Hull MJ, Abraham JL (2002) Aluminum welding fume-induced pneumoconiosis. Hum Pathol 33:819–825

Kao YY, Chen YC, Cheng TJ, Chiung YM, Liu PS (2012) Zinc oxide nanoparticles interfere with zinc ion homeostasis to cause cytotoxicity. Toxicol Sci 125:462–472

Kermanizadeh A, Gaiser BK, Hutchison GR, Stone V (2012) An in vitro liver model–assessing oxidative stress and genotoxicity following exposure of hepatocytes to a panel of engineered nanomaterials. Part Fibre Toxicol 9:28

Lee J, Kang BS, Hicks B, Chancellor TF Jr, Chu BH, Wang HT, Keselowsky BG, Ren F, Lele TP (2008) The control of cell adhesion and viability by zinc oxide nanorods. Biomaterials 29:3743–3749

Mudunkotuwa IA, Rupasinghe T, Wu CM, Grassian VH (2012) Dissolution of ZnO nanoparticles at circumneutral pH: a study of size effects in the presence and absence of citric acid. Langmuir 28:396–403

Nel A, Xia T, Madler L, Li N (2006) Toxic potential of materials at the nanolevel. Science 311:622–627

Rasmussen JW, Martinez E, Louka P, Wingett DG (2010) Zinc oxide nanoparticles for selective destruction of tumor cells and potential for drug delivery applications. Expert Opin Drug Deliv 7:1063–1077

Sano T (1963) Pathology and pathogenesis of pneumoconiosis. Acta Pathol Jpn 13:77–93

Sayes CM, Reed KL, Warheit DB (2007) Assessing toxicity of fine and nanoparticles: comparing in vitro measurements to in vivo pulmonary toxicity profiles. Toxicol Sci 97:163–180

Tsuda H, Fukamachi K, Ohshima Y, Ueda S, Matsuoka Y, Hamaguchi T, Ohnishi T, Takasuka N, Naito A (2005) High susceptibility of human c-Ha-ras proto-oncogene transgenic rats to carcinogenesis: a cancer-prone animal model. Cancer Sci 96:309–316

Valdiglesias V, Costa C, Kilic G, Costa S, Pasaro E, Laffon B, Teixeira JP (2013) Neuronal cytotoxicity and genotoxicity induced by zinc oxide nanoparticles. Environ Int 55:92–100

Warheit DB, Sayes CM, Reed KL (2009) Nanoscale and fine zinc oxide particles: can in vitro assays accurately forecast lung hazards following inhalation exposures? Environ Sci Technol 43:7939–7945

Xia T, Kovochich M, Liong M, Madler L, Gilbert B, Shi H, Yeh JI, Zink JI, Nel AE (2008) Comparison of the mechanism of toxicity of zinc oxide and cerium oxide nanoparticles based on dissolution and oxidative stress properties. ACS Nano 2:2121–2134

Xu J, Futakuchi M, Iigo M, Fukamachi K, Alexander DB, Shimizu H, Sakai Y, Tamano S, Furukawa F, Uchino T, Tokunaga H, Nishimura T, Hirose A, Kanno J, Tsuda H (2010) Involvement of macrophage inflammatory protein 1 alpha (MIP 1 alpha) in promotion of rat lung and mammary carcinogenic activity of nanoscale titanium dioxide particles administered by intra-pulmonary spraying. Carcinogenesis 31:927–935

Yang H, Liu C, Yang D, Zhang H, Xi Z (2009) Comparative study of cytotoxicity, oxidative stress and genotoxicity induced by four typical nanomaterials: the role of particle size, shape and composition. J Appl Toxicol 29:69–78

Carcinogenicity of perfluorooctanoic acid, tetrafluoroethylene, dichloromethane, 1,2-dichloropropane, and 1,3-propane sultone

Published Online
July 11, 2014
http://dx.doi.org/10.1016/S1470-2045(14)70316-X

For more on the **IARC Monographs** see http://monographs.iarc.fr/

Upcoming meetings
Sept 30–Oct 7, 2014
Volume 111: Some nanomaterials and some fibres;
March 3–10, 2015
Volume 112: Some organophosphate insecticides

Monograph Working Group Members
I I Rusyn (USA)–Meeting Chair; L Fritschi (Australia); C M Sergi (Canada); J Hansen (Denmark); F Le Curieux (Finland); H M Bolt (Germany); S Fukushima, G Ichihara, K Kamae, S Kumagai, H Tsuda (Japan); K Kjaerheim (Norway); S M Bartell, M F Cesta, W Chiu, G Cooper, J C DeWitt, M Friesen, L H Lash, K Steenland (USA)

Declaration of interests
SMB has received research funding from the C8 class action settlement agreement between DuPont and plaintiffs; funds were administered by the Garden City Group that reports to the court (SMB's work was independent of either party in the lawsuit). SMB has also received funding from the National Institutes of Health, the California Air Resources Board, and the US Environmental Protection Agency.

Invited specialists
J W Cherrie (UK)

Declaration of interests
JWC has received research funding from the Association of Plastic Manufacturers Europe until 2012, European Chemical Industry Council, European

In June, 2014, 20 experts from nine countries met at the International Agency for Research on Cancer (IARC; Lyon, France) to assess the carcinogenicity of perfluorooctanoic acid (PFOA), tetrafluoroethylene (TFE), dichloromethane (DCM), 1,2-dichloropropane (1,2-DCP), and 1,3-propane sultone (1,3-PS). These assessments will be published as volume 110 of the IARC Monographs.[1]

1,2-DCP is a synthetic chlorinated solvent, and a byproduct of the production of epichlorohydrin. It is used mainly as a chemical intermediate in the production of other organic chemicals such as propylene, carbon tetrachloride, and tetrachloroethylene, and in paint stripping, and was used as an ink-removal agent in the printing industry in Japan from the mid-1990s until 2012. 1,2-DCP was classified as carcinogenic to humans (Group 1), on the basis of sufficient evidence in humans that exposure to 1,2-DCP causes cholangiocarcinoma (biliary-tract cancer). The most important human evidence regarding carcinogenicity comes from studies of workers in a small offset printing plant in Osaka, Japan, where a very high risk of cholangiocarcinoma was reported.[2,3] Additional cases were later identified from several other printing plants. The major challenge in assessing the occurrence of cancer in the Japanese printing plants was to establish whether the observed excess of cholangiocarcinoma could be attributed to a specific agent. Although workers were exposed to more than 20 different chemicals, exposure to 1,2-DCP was common to all except one of the 24 patients with cholangiocarcinoma, and six of the patients had no known exposure to DCM (used together with 1,2-DCP in this industry). The working group considered the rarity of cholangiocarcinoma, the very high relative risk, the young ages of the patients, the absence of non-occupational risk factors, and the intensity of the exposure as indications that the excess of cholangiocarcinoma was unlikely to be the result of chance, bias, or non-occupational confounding. Sufficient evidence for carcinogenicity has also been reported in experimental animals, with malignant lung and hepatocellular tumours observed in exposed mice.[4,5] On the basis of this evidence, most of the working group concluded that 1,2-DCP was the causative agent responsible for the large excess of cholangiocarcinoma in the exposed workers. However, a minority concluded that the association between 1,2-DCP and cholangiocarcinoma was credible, but the role of other agents, mainly DCM, could not be separated with complete confidence. The working group members also noted that most of the evidence came from reports in just one plant.

DCM has been used in the manufacture of polycarbonate plastics, hydrofluorocarbons, synthetic fibres, and photographic films, as an aerosol propellant, for paint stripping, metal cleaning, and printing-ink removal, and as an extraction solvent for some foods. DCM was classified as probably carcinogenic to humans (Group 2A) on the basis of limited evidence that it causes biliary-tract cancer and non-Hodgkin lymphoma in humans and sufficient evidence of carcinogenicity in experimental animals (malignant lung and hepatocellular tumours in male and female mice).[2,3,6–9] In making its overall assessment, the working group also took into account the strong evidence that DCM metabolism via glutathione-*S*-transferase T1 (GSTT1) leads to the formation of reactive metabolites, that GSTT1 activity is strongly associated with genotoxicity of DCM in vitro and in vivo, and that GSTT1-mediated metabolism of DCM does occur in humans.

TFE is used mainly as an intermediate in the production of polytetrafluoroethylene, with application in a wide range of industrial and consumer products, including non-stick coatings and waterproof clothing. Despite the absence of adequate data on cancer in humans and weak mechanistic information, the working group's overall assessment of the carcinogenicity of TFE was upgraded from possibly carcinogenic to humans (Group 2B) to probably carcinogenic (Group 2A), on the basis of sufficient evidence in experimental animals with a striking and atypical pattern of tumours. Specifically, neoplasms at several sites and with very high incidence were noted in male and female rodents after exposure to TFE (mice: liver haemangiosarcoma, hepatocellular carcinoma, and histocytic sarcoma; rats: renal cell adenoma or carcinoma, hepatocellular carcinoma, mononuclear cell leukaemia, and the rare liver haemangiosarcoma [in female rats only]).[10]

1,3-PS has been used as an intermediate in the manufacture of other chemicals and a range of products including detergents, pesticides, pharmaceuticals, and photographic materials. Major industrial use has been largely terminated, but use in manufacturing lithium batteries has been reported recently. 1,3-PS was classified as probably carcinogenic to humans

(Group 2A), on the basis of inadequate evidence in humans and sufficient evidence in experimental animals with a mechanistic upgrade supported by strong evidence of genotoxicity. 1,3-PS causes malignant tumours of the skin and lymphohaematopoietic system in mice and malignant glioma in rats.[11,12] 1,3-PS is an alkylating agent that reacts directly with DNA and protein. DNA reactivity was evident in various genotoxicity assays, including in animals and in human cells in vitro. Because 1,3-PS does not require metabolic activation and reacts directly with DNA and other macromolecules, the working group concluded that this mechanism probably operates both in animals and humans.

PFOA and its salts are used in the production of fluoropolymers and in many industrial and commercial products, notably in producing non-stick cookware, waterproof clothing, and paper coatings used in food packaging. PFOA is persistent in the environment and has been detected worldwide at low concentrations in the general population. Additionally, communities near some production facilities have been highly exposed to PFOA as a result of emissions to air and water. On the basis of limited evidence in humans that PFOA causes testicular and renal cancer, and limited evidence in experimental animals, the working group classified PFOA as possibly carcinogenic to humans (Group 2B). Increased risk of kidney cancer with a statistically significant exposure–response trend was reported in workers in a fluoropolymer production plant in West Virginia, USA, and in an exposed community near the plant (relative risk 2·0, 95% CI 1·0–3·9).[13,14] Increases of about threefold in the risk of testicular cancer were reported in the most highly exposed residents of communities near the same plant.[14,15] The working group considered the evidence regarding mechanisms of PFOA-associated carcinogenesis to be moderate, which did not lead to a change in the overall classification of PFOA.

We declare no competing interests.

Lamia Benbrahim-Tallaa, Béatrice Lauby-Secretan, Dana Loomis, Kathryn Z Guyton, Yann Grosse, Fatiha El Ghissassi, Véronique Bouvard, Neela Guha, Heidi Mattock, Kurt Straif, on behalf of the International Agency for Research on Cancer Monograph Working Group

International Agency for Research on Cancer, Lyon, France

1 International Agency for Research on Cancer. Volume 110: Perfluoro-octanoic acid, tetrafluoroethylene, dichloromethane, 1,2-dichloropropane, 1,3-propane sultone. IARC Working Group; Lyon, June 3–10, 2014. *IARC Monogr Eval Carcinog Risk Chem Hum* (in press).

2 Kumagai S, Kurumatani N, Arimoto A, Ichihara G. Cholangiocarcinoma among offset colour proof-printing workers exposed to 1,2-dichloropropane and/or dichloromethane. *Occup Environ Med* 2013; **70:** 508–10.

3 Kubo S, Nakanuma Y, Takemura S, et al. Case series of 17 patients with cholangiocarcinoma among young adult workers of a printing company in Japan. *J Hepatobiliary Pancreat Sci* 2014; **21:** 479–88.

4 National Toxicology Program. NTP toxicology and carcinogenesis studies of 1,2-dichloropropane (propylene dichloride) (CAS no. 78-87-5) in F344/N rats and B6C3F1 mice (gavage studies). *Natl Toxicol Program Tech Rep Ser* 1986; **263:** 1–182.

5 Matsumoto M, Umeda Y, Take M, Nishizawa T, Fukushima S. Subchronic toxicity and carcinogenicity studies of 1,2-dichloropropane inhalation to mice. *Inhal Toxicol* 2013; **25:** 435–43.

6 Lanes SF, Rothman KJ, Dreyer NA, Soden KJ. Mortality update of cellulose fiber production workers. *Scand J Work Environ Health* 1993; **19:** 426–28.

7 Gibbs GW, Amsel J, Soden K. A cohort mortality study of cellulose triacetate-fiber workers exposed to methylene chloride. *J Occup Environ Med* 1996; **38:** 693–97.

8 Wang R, Zhang Y, Lan Q, et al. Occupational exposure to solvents and risk of non-Hodgkin lymphoma in Connecticut women. *Am J Epidemiol* 2009; **169:** 176–85.

9 National Toxicology Program. NTP toxicology and carcinogenesis studies of dichloromethane (methylene chloride) (CAS no. 75-09-2) in F344/N rats and B6C3F$_1$ mice (inhalation studies). *Natl Toxicol Program Tech Rep Ser* 1986; **306:** 1–208.

10 National Toxicology Program. NTP toxicology and carcinogenesis studies of tetrafluoroethylene (CAS no. 116-14-3) in F344 rats and B6C3F1 mice (inhalation studies). *Natl Toxicol Program Tech Rep Ser* 1997; **450:** 1–321.

11 Doak SM, Simpson BJ, Hunt PF, Stevenson DE. The carcinogenic response in mice to the topical application of propane sultone to the skin. *Toxicology* 1976; **6:** 139–54.

12 Weisburger EK, Ulland BM, Nam J, Gart JJ, Weisburger JH. Carcinogenicity tests of certain environmental and industrial chemicals. *J Natl Cancer Inst* 1981; **67:** 75–88.

13 Steenland K, Woskie S. Cohort mortality study of workers exposed to perfluorooctanoic acid. *Am J Epidemiol* 2012; **176:** 909–17.

14 Vieira VM, Hoffman K, Shin HM, Weinberg JM, Webster TF, Fletcher T. Perfluorooctanoic acid exposure and cancer outcomes in a contaminated community: a geographic analysis. *Environ Health Perspect* 2013; **121:** 318–23.

15 Barry V, Winquist A, Steenland K. Perfluorooctanoic acid (PFOA) exposures and incident cancers among adults living near a chemical plant. *Environ Health Perspect* 2013; **121:** 1313–18.

Solvents Industry Group, Shell, and Concawe (the oil industry association for environment, health, and safety).

Representatives
M Bisson, for INERIS (Institut National de l'Environnement Industriel et des Risques, France)

Observers
J Arts, for the REACH Chlorsolv Consortium and the European Chlorinated Solvent Association and the Halogenated Solvents Industry Alliance (Netherlands); J L Butenhoff, for the PlasticsEurope Fluoropolymers Group (USA); J Carretier, for the Léon Bérard Centre (France); A Forrest, for the United Fire Fighters of Winnipeg (Canada); G W Olsen, for the Center for Advancing Risk Assessment Science and Policy of the American Chemistry Council (USA); J M Symons IV, for the PlasticsEurope Fluoropolymers Group (USA)

Declaration of interests
JA is employed by AkzoNobel. JLB is retired but employed (part-time) by 3M; receives a pension, benefits, and travel support from 3M; and holds stock in 3M. GWO is employed by 3M; receives travel support from 3M; and holds stock in 3M. JMS is employed by DuPont.

IARC/WHO secretariat
L Benbrahim-Tallaa; V Bouvard; F El Ghissassi; Y Grosse; N Guha; K Z Guyton; B Lauby-Secretan; D Loomis; H Mattock; M Olivier; A Shapiro; K Straif; F Sylla; A Takeuchi; I Zastenskaya; J Zavadil

Carcinogenicity of fluoro-edenite, silicon carbide fibres and whiskers, and carbon nanotubes

In October, 2014, 21 experts from ten countries met at the International Agency for Research on Cancer (IARC; Lyon, France) to assess the carcinogenicity of fluoro-edenite, silicon carbide (SiC) fibres and whiskers, and carbon nanotubes (CNTs) including single-walled (SWCNTs) and multi-walled (MWCNTs) types. These assessments will be published as Volume 111 of the IARC Monographs.[1]

Fluoro-edenite was first identified around the Etna volcano near Biancavilla, Italy; a similar mineral was also reported from the Kimpo volcano in Japan. Fluoro-edenite can occur as asbestiform fibres. Unpaved roads made from local quarry products from Biancavilla, used since the 1950s, are a source for airborne fluoro-edenite fibres; additionally indoor air was also contaminated from the use of the quarry's products in building materials. Several surveillance studies reported an excess of mesothelioma incidence and mortality in the regional population of Biancavilla.[2] Since the rate ratios for mesothelioma were large and stable, chance was unlikely to explain these findings. The excess was similar in men and women, and most prominent in young adults, suggesting an environmental rather than occupational cause. Moreover, most of the cases had no history of occupational exposure to asbestos. Fluoro-edenite fibrous amphibole was classified as carcinogenic to humans (Group 1) on the basis of sufficient evidence in humans that exposure to fluoro-edenite causes mesothelioma. Sufficient evidence of carcinogenicity was also reported in experimental animals, with increased incidences of mesotheliomas observed in one study in male and female rats given fibrous fluoro-edenite by intraperitoneal or intrapleural injection.[3] The results of the few available mechanistic studies were consistent with proposed mechanisms of fibre carcinogenicity.[4]

SiC occurs in several forms: particles, fibres, and whiskers. SiC particles are manufactured (mostly for use as industrial abrasive) mainly by the Acheson process, with SiC fibres being unwanted by-products. SiC fibres are generally poly-crystalline; of variable length and diameter, and may include fibres that are indistinguishable from whiskers. SiC whiskers are intentionally produced by different processes as durable industrial substitutes for asbestos; they are physically homogeneous and mono-crystalline, and their dimensions are similar to asbestos amphiboles. The carcinogenicity of SiC fibres was investigated in two cohorts of Acheson process workers who were exposed to fibrous and non-fibrous SiC, quartz, and cristobalite. In a Canadian cohort study,[5] an excess of lung cancer mortality was observed. An excess of lung cancer and an exposure–response relationship with SiC fibres was described in the most detailed report from a series of studies on cancer incidence in a Norwegian cohort.[6] The analyses were limited to workers with at least 3 years of employment in the plant and based on a detailed job-exposure matrix taking into account multiple exposures. The exposure–response relationship was somewhat weakened after adjustment for exposure to cristobalite. Occupational exposures associated with the Acheson process were classified as carcinogenic to humans (Group 1) on the basis of sufficient evidence in humans that they cause lung cancer. Since the correlation between exposures to SiC fibres and cristobalite made it difficult to disentangle their independent effects, the Working Group concluded that fibrous SiC is possibly carcinogenic to humans (Group 2B) based on limited evidence in humans that it causes lung cancer. No data on cancer in humans exposed to SiC whiskers were available. In experimental animals, there was sufficient evidence for the carcinogenicity of SiC whiskers, with mesotheliomas observed in three studies in female rats treated by intrapleural implantation,[7] intrapleural injection, or intraperitoneal injection, and in one inhalation study in rats that did not include concurrent controls. Although not unanimous, the Working Group classified SiC whiskers as probably carcinogenic to humans (Group 2A) rather than possibly carcinogenic to humans (Group 2B), on the basis that the physical properties of the whiskers resemble those of asbestos and erionite fibres, which are known carcinogens. In addition, the results of available mechanistic studies were consistent with proposed mechanisms of fibre carcinogenicity.[4] The majority of the Working Group considered that differences in the nature of SiC fibres and SiC whiskers warranted separate evaluations.

Carbon nanotubes may consist of either a single graphene cylinder (SWCNTs) with an outer diameter of 1–3 nm, or of multiple graphene cylinders arranged in concentric layers (MWCNTs) with diameters of 10–200 nm. CNTs are typically few micrometres in length, ranging from a few hundreds of nanometres to several tens of micrometres; their physical and chemical characteristics vary depending on the production technique. Applications include improving the structural properties of fabrics, plastics, rubbers, electronics, and composite materials. The highest release of CNTs, usually as entangled agglomerates which can be respirable, is observed during production and handling, and in cleaning of the production reactor. Measurement of occupational exposure is limited,

Published Online
October 31, 2014
http://dx.doi.org/10.1016/S1470-2045(14)71109-X

For more on the **IARC Monographs** see http://monographs.iarc.fr/

Upcoming meetings

March 3–10, 2015, Volume 112: Some organophosphate insecticides and herbicides: diazinon, glyphosate, malathion, parathion, and tetraclorvinphos

June 2–9, 2015, Volume 113: Some organochlorine insecticides and some chlorphenoxy herbicides

IARC Monograph Working Group Members

A B Kane (USA)—Meeting Chair; M Debia; C Dion (Canada); P Møller (Denmark); K Savolainen (Finland); I Gusava Canu; M C Jaurand (France); P Comba; B Fubini (Italy); N Kobayashi; Y Morimoto; H Tsuda (Japan); I J Yu (South Korea); R Vermeulen (Netherlands); M D Bugge (Norway); T F Bateson; E D Kuempel; D L Morgan; K E Pinkerton; L M Sargent; L Stayner (USA)

Invited Specialists

None

Representatives

A Ben Amara, National Agency for Sanitary and Environmental Product Control, Tunisia; M E Gouze; N Thieriet, for the French Agency for Food, Environment and Occupational Health and Safety, France

Observers

N Falette, for the Léon Bérard Centre, France; S Føreland, Observer for Silicon Carbide Manufacturers Association (SiCMa), Luxemburg; J Muller-Bondue, Observer for Nanocyl SA, Belgium

IARC/WHO Secretariat
L Benbrahim-Tallaa; N Guha; V Bouvard; R Carel; F El Ghissassi; Y Grosse; K Z Guyton; B Lauby-Secretan; D Loomis; H Mattock; C Scoccianti; K Straif

and consumer exposure was not quantified. No human cancer data were available to the Working Group, indicating inadequate evidence for the carcinogenicity of CNTs in humans. Some CNTs were tested in rodents. MWCNT-7 caused peritoneal mesotheliomas in male and female rats in one intraperitoneal injection study[8] and one intrascrotal injection study,[9] and in male $p53^{+/-}$ mice in two intraperitoneal injection studies.[10] Inhalation of MWCNT-7 promoted bronchioloalveolar adenoma and carcinoma in male mice.[11] In one intraperitoneal study, two other types of MWCNTs with physical dimensions similar to those of MWCNT-7 (length, 1–19 μm; diameter, 40–170 nm) caused mesotheliomas in male and female rats.[8] Two studies with SWCNTs in rats were inconclusive. Regarding carcinogenicity in experimental animals, the Working Group concluded that there was sufficient evidence for MWCNT-7, limited evidence for the two other types of MWCNTs with dimensions similar to MWCNT-7, and inadequate evidence for SWCNTs. Mechanistic and other data in rodents provided evidence of translocation of three types of MWCNTs (including MWCNT-7) to the pleura.[12] Additionally, inhalation of some MWCNTs or SWCNTs induced acute or persistent pulmonary inflammation, granuloma formation, fibrosis, and bronchiolar or bronchioloalveolar hyperplasia in rodents.[13,14] Studies in rodents (eg, Shvedova et al[15]) and in cultured human lung or mesothelial cells showed that MWCNTs, SWCNTs, or both induce genetic lesions such as DNA strand breaks, oxidised DNA bases, mutations, micronucleus formation, and chromosomal aberrations. SWCNTs and MWCNTs also perturb the cellular mitotic apparatus, including microtubules and centrosomes, in human lung epithelial cells.[16,17] As a whole, the Working Group acknowledged that the above mechanisms are all relevant to humans. However, a majority did not consider the mechanistic evidence for carcinogenicity—especially concerning chronic endpoints—to be strong for any specific CNT. Furthermore, the lack of coherent evidence across the various distinct CNTs precluded generalisation to other types of CNTs. Thus, MWCNT-7 was classified as possibly carcinogenic to humans (Group 2B); and SWCNTs and MWCNTs excluding MWCNT-7 were categorised as not classifiable as to their carcinogenicity to humans (Group 3).

We declare no competing interests.

Yann Grosse, Dana Loomis, Kathryn Z Guyton, Béatrice Lauby-Secretan, Fatiha El Ghissassi, Véronique Bouvard, Lamia Benbrahim-Tallaa, Neela Guha, Chiara Scoccianti, Heidi Mattock, Kurt Straif, on behalf of the International Agency for Research on Cancer Monograph Working Group

International Agency for Research on Cancer, Lyon, France

1 International Agency for Research on Cancer. Volume 111: Fluoro-edenite, silicon carbide fibres and whiskers, and single-walled and multi-walled carbon nanotubes IARC Working Group. Lyon; 30 Sep–7 Oct 2014. *IARC Monogr Eval Carcinog Risk Chem Hum* (in press).

2 Bruno C, Tumino R, Fazzo L, et al. Incidence of pleural mesothelioma in a community exposed to fibres with fluoro-edenitic composition in Biancavilla (Sicily, Italy). *Ann Ist Super Sanita* 2014; **50:** 111–18.

3 Belpoggi F, Tibaldi E, Lauriola M, et al. The efficacy of long-term bioassays in predicting human risks: mesotheliomas induced by fluoro-edenitic fibres present in lava stone from Etna Volcano in Biancavilla Italy. *Eur J Oncol* 2014; **16:** 185–95.

4 International Agency for Research on Cancer. Volume 100C: Arsenic, metals, fibres, and dusts. IARC Working Group. Lyon; 17–24 March 2009. *IARC Monogr Eval Carcinog Risk Chem Hum* 2012; **100C:** 219–316.

5 Infante-Rivard C, Dufresne A, Armstrong B, Bouchard P, Thériault G. Cohort study of silicon carbide production workers. *Am J Epidemiol* 2014; **140:** 1009–15.

6 Bugge MD, Kjærheim K, Føreland S, Eduard W, Kjuus H. Lung cancer incidence among Norwegian silicon carbide industry workers: associations with particulate exposure factors. *Occup Environ Med* 2012; **69:** 527–33.

7 Johnson NF, Hahn FF. Induction of mesothelioma after intrapleural inoculation of F344 rats with silicon carbide whiskers or continuous ceramic filaments. *Occup Environ Med* 1996; **53:** 813–16.

8 Nagai H, Okazaki Y, Chew SH, Misawa N, Yamashita Y, Akatsuka S, et al. Diameter and rigidity of multiwalled carbon nanotubes are critical factors in mesothelial injury and carcinogenesis. *Proc Natl Acad Sci USA* 2011; **108:** E1330–38.

9 Sakamoto Y, Nakae D, Fukumori N, et al. Induction of mesothelioma by a single intrascrotal administration of multi-wall carbon nanotube in intact male Fischer 344 rats. *J Toxicol Sci* 2009; **34:** 65–76.

10 Takagi A, Hirose A, Futakuchi M, Tsuda H, Kanno J. Dose-dependent mesothelioma induction by intraperitoneal administration of multi-wall carbon nanotubes in p53 heterozygous mice. *Cancer Sci* 2012; **103:** 1440–44.

11 Sargent LM, Porter DW, Staska LM, et al. Promotion of lung adenocarcinoma following inhalation exposure to multi-walled carbon nanotubes. *Part Fibre Toxicol* 2014; **11:** 3.

12 Mercer RR, Scabilloni JF, Hubbs AF, et al. Distribution and fibrotic response following inhalation exposure to multi-walled carbon nanotubes. *Part Fibre Toxicol* 2013; **10:** 33.

13 Shvedova AA, Kisin E, Murray AR, et al. Inhalation vs. aspiration of single-walled carbon nanotubes in C57BL/6 mice: inflammation, fibrosis, oxidative stress, and mutagenesis. *Am J Physiol Lung Cell Mol Physiol* 2008; **295:** L552–65.

14 Pauluhn J. Subchronic 13-week inhalation exposure of rats to multiwalled carbon nanotubes: toxic effects are determined by density of agglomerate structures, not fibrillar structures. *Toxicol Sci* 2010; **113:** 226–42.

15 Shvedova AA, Yanamala N, Kisin ER, et al. Long-term effects of carbon containing engineered nanomaterials and asbestos in the lung: one year postexposure comparisons. *Am J Physiol Lung Cell Mol Physiol* 2014; **306:** L170–82.

16 Sargent LM, Hubbs AF, Young SH, et al. Single-walled carbon nanotube-induced mitotic disruption. *Mutat Res* 2012; **745:** 28–37.

17 Siegrist KJ, Reynolds SH, Kashon ML, et al. Genotoxicity of multi-walled carbon nanotubes at occupationally relevant doses. *Part Fibre Toxicol* 2014; **11:** 1–15.